PROCEEDINGS OF SCIENCE

Neutrino Oscillation Parameter Measurements

Zhe Wang[a,*]

[a] *Department of Engineering Physics, Tsinghua University, Beijing 100084, China*

E-mail: wangzhe-hep@mail.tsinghua.edu.cn

In this paper recording my presentation at the ICHEP 2020, I summarize the recent experimental progress on the measurements of the neutrino mixing parameters, θ_{13}, θ_{23}, θ_{12}, Δm^2_{12}, and $|\Delta m^2_{13}|$. I will also briefly mention the anomalies in the neutrino oscillation study.

40th International Conference on High Energy physics - ICHEP2020
July 28 - August 6, 2020
Prague, Czech Republic (virtual meeting)

*Speaker

https://pos.sissa.it/

PoS(ICHEP2020)044

1. Introduction

The earlier measured deficit of solar neutrino flux (Homestake, GALLEX/GNO, SAGE) to prediction (J. Bahcall) is the trigger of many modern neutrino oscillation experiments. With the proof of solar neutrino total flux measurement (SNO) and atmospheric neutrino deficit result (Super-Kamiokande), massive neutrinos became the first evidence beyond the standard model.

The PMNS matrix is a 3×3 matrix used to describe the connection between neutrino mass eigenstates and flavor eigenstates. It consists of three mixing angles, θ_{13}, θ_{23}, θ_{12}, and one phase angle, δ, for Dirac neutrinos. Together with the mass differences between mass eigenstates $\Delta m^2_{ij} = m^2_i - m^2_j$, Δm^2_{12} and Δm^2_{13} (or Δm^2_{23}), we can predict the transition probability of neutrinos between two flavors. If neutrinos travel through dense matters, like the Sun or Earth, the matter, i.e. MSW, effect should be also taken into account.

At the same time, there are also signs that experiments are not perfectly consistent with the 3×3 scheme. It could be experimental or theoretical uncertainties, or it is due to a new generation of neutrinos, sterile neutrinos.

In this proceeding, I will summarize the recent progress on the measurements of the mixing parameters, θ_{13}, θ_{23}, θ_{12}, Δm^2_{12}, and $|\Delta m^2_{13}|$, while, for the CP phase, δ and the sign of Δm^2_{13}, it will be discussed in detail in Ichikawa's talk of the same ICHEP 2020 series [1]. I will also briefly mention the anomalies in neutrino oscillation studies and sterile neutrino searching.

2. Three Generations

In the three-generation framework, according to their sensitive regions, the experiments are categorized as 1) reactor neutrino experiments with baseline less than 2 km for θ_{13} and Δm^2_{ee} (explained later), 2) solar neutrino experiments and the KamLAND reactor neutrino experiment for θ_{12} and Δm^2_{21}, and 3) atmospheric and accelerator neutrino experiments, for θ_{23}, Δm^2_{31}, θ_{13} and δ.

2.1 Reactor Neutrino Experiments (baseline<2 km)

In this section, the recent results of the Daya Bay, RENO, and Double Chooz reactor neutrino experiments will be discussed. Reactors are powerful $\bar{\nu}_e$ sources through nuclear fissions. Neutrino energy from reactors is in the range of 0-10 MeV with neutrino energy peak around 3-4 MeV if convoluted with the detection cross-section. With 1-2 km long baseline, the range of L/E makes the experiments appropriate for the θ_{13} and Δm^2_{31} determination.

The equation of reactor $\bar{\nu}_e$ survival probability, P_{ee}, is [2]

$$\begin{aligned} P_{ee} =& 1 - \cos^4\theta_{13}\sin^2 2\theta_{12}\sin^2\Delta_{21} \\ & - \sin^2 2\theta_{13}(\cos^2\theta_{12}\sin^2\Delta_{31} + \sin^2\theta_{12}\sin^2\Delta_{32}) \\ =& 1 - \cos^4\theta_{13}\sin^2 2\theta_{12}\sin^2\Delta_{21} - \sin^2 2\theta_{13}\sin^2\Delta m^2_{ee}, \end{aligned} \tag{1}$$

where

$$\Delta_{ij} = \Delta m^2_{ij}(\mathrm{eV}^2)\mathrm{L(m)/E(MeV)}, \tag{2}$$

and the term in the parenthesis is shortened as $\sin^2\Delta m^2_{ee}$ in the last line of Eq. (1).

PoS(ICHEP2020)044

The $\bar{\nu}_e$'s are detected through the inverse-beta-decay,

$$\bar{\nu}_e + p \rightarrow e^+ + n, \tag{3}$$

followed by neutron capture on hydrogen or gadolinium

$$\begin{aligned} n + p &\rightarrow \mathrm{D} + \gamma \ (2.2\ \mathrm{MeV}), \\ n + \mathrm{Gd} &\rightarrow \mathrm{Gd}^* + \gamma' \mathrm{s} \ (8\ \mathrm{MeV}). \end{aligned} \tag{4}$$

The sequential e^+ and n-capture signals form a prompt-delayed signal pair. The average capture time is about 200 μs in liquid scintillator and about 30 μs in Gd-doped (0.1% by mass) liquid scintillator. The process greatly enhanced the signal-to-background ratio and decreased the request of the level of radioactive background for these experiments. The energy of the neutrino can be derived by the e^+ energy.

The three experiments all have taken a strategy of using multiple identical detectors at near and far experimental sites so that the critical systematic uncertainties can cancel, like reactor power and detection efficiency.

The recent θ_{13} and Δm^2_{ee} results from the Daya Bay, RENO, and Double Chooz are summarized in Table. 1. The results from different statistical datasets, i.e. neutron capture on Gd or H, are separated. All results are consistent with their uncertainties.

Table 1: The recent θ_{13} and Δm^2_{ee} results from the Daya Bay, RENO, and Double Chooz experiments. The nGd dataset is for neutron capture on Gd and the nH dataset is for neutron capture on H, and the total capture includes both of them.

Experiment and dataset	$\sin^2 2\theta_{13}$	$\lvert\Delta m^2_{ee}\rvert$
Daya Bay nGd [2]	0.0856 ± 0.0029	$(2.52 \pm 0.07) \times 10^{-3}$ eV^{-3}
Daya Bay nH [3]	0.071 ± 0.011	-
RENO nGd [4]	0.0892 ± 0.0063	$(2.74 \pm 0.12) \times 10^{-3}$ eV^{-3}
RENO nH [5]	0.086 ± 0.016	-
Double Chooz total capture [6]	0.102 ± 0.012	-

2.2 Solar Neutrino Experiments and KamLAND

Neutrinos from the solar fusion processes are ν_e. Below 2 MeV are *pp*, Be7, *pep*, and CNO neutrinos, and between 2 - 20 MeV are B8 and *hep* neutrinos, in which the names are given according to their fusion process.

For the solar neutrinos transition probability, the matter effect must be considered. The full solar ν_e survival probability can be descibed by the following equations [7],

$$P_{ee} = \cos^4\theta_{13}\left(\frac{1}{2} + \frac{1}{2}\cos 2\theta^M_{12}\cos 2\theta_{12}\right), \tag{5}$$

where the mixing angle in matter is

$$\cos 2\theta^M_{12} = \frac{\cos 2\theta_{12} - \beta}{\sqrt{(\cos 2\theta_{12} - \beta)^2 + \sin^2 2\theta_{12}}}, \tag{6}$$

with

$$\beta = \frac{2\sqrt{2}G_F \cos^2\theta_{13} n_e E_\nu}{\Delta m^2_{21}}. \tag{7}$$

At high energy (> 10 MeV), the transition is dominated by matter effect and the P_{ee} is about 0.3, while at low energy (< 2 MeV), neutrino is like traveling in vacuum and P_{ee} is about 0.5. In between, there should be a smooth transition, the so-called 'upturn' effect. Due to the matter effect, the sign of the Δm^2_{21} is determined to be positive. On the Earth, if the solar ν_e is detected in the evening, the survival probability is going to be altered again by a few percent due to the Earth matter effect.

Originally, solar neutrinos were detected by a few radiochemical exepriments, Homestake, GALLEX/GNO, and SAGE. They detected solar neutrinos through the charged current, CC, processes,

$$\begin{aligned} \nu_e + {}^{37}\mathrm{Cl} &\to {}^{37}\mathrm{Ar} + \mathrm{e}^- \text{ (CC)}, \\ \nu_e + {}^{71}\mathrm{Ga} &\to {}^{71}\mathrm{Ge} + \mathrm{e}^- \text{ (CC)}. \end{aligned} \tag{8}$$

The Super-Kamiokande and Borexino experiments detect solar neutrinos through neutrino-electron elastic scattering, ES,

$$\nu_x + e^- \to \nu_x + e^- \text{ (ES)}. \tag{9}$$

The ES process can be triggered by ν_x which includes ν_e, ν_μ and ν_τ. At the solar neutrino energy, the ES process signals including roughly 80% of CC events and 20% of neutral current, NC, events.

The SNO experiment, however, can measure solar ν_e through CC and NC processes on deuterons and the same ES process on electrons. The CC and NC processes are

$$\begin{aligned} \nu_e + d &\to p + p + e^- \text{ (CC)}, \\ \nu_x + d &\to p + n + \nu_x \text{ (NC)}. \end{aligned} \tag{10}$$

The solar neutrino experiments measure the oscillation parameters of θ_{12} and Δm^2_{21}. The SNO experiments still hold the best independent measurement of NC measurement, i.e. total B8 neutrino flux.

KamLAND is also a reactor neutrino experiment, but, with typical baseline of 180 kilometers, is sensitive the reactor $\bar{\nu}_e$ oscillation dominated by the θ_{12} and Δm^2_{21} term in Eq. 1. Assuming a CPT invariance, their measurement can be compared with the solar neutrino experiments.

In [8], the Super-Kamiokande experiment reported their new solar neutrino results and its combinations with the SNO experiments and KamLAND as shown in Tab. 2. The discrepancy between SK+SNO fit and KamLAND result has decreased to 1.4 σ from 2 σ. The signature of the upturn is not very strong and it disfavors a flat oscillation probability by about 1 σ. A day-night difference is

$$A^{Fit}_{DN} = (-2.1 \pm 1.1)\% \; [3.5 < E < 19.5 \text{ (MeV)}]. \tag{11}$$

Table 2: The latest solar neutrino measurement [8] by KamLAND, the combination of Super-Kamiokande and SNO experiments, and the combination with all of them.

Experiment	$\sin^2(\theta_{12})$	Δm^2_{21} $[10^{-5}\ eV^2]$
KamLAND	$0.316^{+0.034}_{-0.026}$	$7.54^{+0.19}_{-0.18}$
SK+SNO	0.306 ± 0.014	$6.11^{+1.21}_{-0.68}$
Combined	$0.306^{+0.013}_{-0.012}$	$7.51^{+0.19}_{-0.18}$

2.3 Atmospheric and Accelerator Neutrino Experiments

Atmospheric neutrinos are generated by the pion, kaon and muon decays after cosmic-ray protons hitting atmospheric molecules, for example:

$$\begin{aligned} \pi^- &\to \mu^- + \bar{\nu}_\mu, \\ K^+ &\to \mu^+ + \nu_\mu, \\ \mu^- &\to e^- + \bar{\nu}_e + \nu_\mu. \end{aligned} \tag{12}$$

The initial flavor contents are ν_e, $\bar{\nu}_e$, ν_μ, and $\bar{\nu}_\mu$. The main energy range of the atmospheric neutrinos is from 0.1 to 10 GeV. Their flux is predicted by [9] and [10]. Particularly the ratio of $\frac{\nu_\mu+\bar{\nu}_\mu}{\nu_e+\bar{\nu}_e}$ is well predicted and is about 2 in a large range.

Atmospheric neutrinos come from all the ways of the Earth, they can come directly from the air upon us, or they can pass through the whole diameter of the Earth. Their baselines are 10-12000 km.

Accelerator neutrinos are generated with a proton beam hitting a target. Charged pion products are collimated with a horn system. Accelerator neutrinos are dominantly ν_μ, and $\bar{\nu}_\mu$, but with some ν_e, $\bar{\nu}_e$ contaminations. The particle and anti-particle species can be selected by the current of the horn system. Their energies are in the GeV range. With an off-axis technical, it makes the neutrino energy spread much smaller and to peak at the interested range for some parameter measurement.

The oscillation formula for the accelerator neutrinos can be found, for example, in [11, 12]. The atmospheric neutrino can go through the more complicated Earth structures than accelerator neutrinos and analytic calculation is needed [13]. The ν_μ and $\bar{\nu}_\mu$ oscillation patterns of accelerator and atmospheric neutrinos are shown in Fig. 1. In the $\nu_\mu \to \nu_\mu$ or $\bar{\nu}_\mu \to \bar{\nu}_\mu$ channel, with θ_{13} input, the neutrino survival probability is sensitive to the measurement of θ_{23} and the magnitude of Δm^2_{31}. In the $\nu_\mu \to \nu_e$ or $\bar{\nu}_\mu \to \bar{\nu}_e$ channel, the oscillation probability measurement is sensitive to a combination of θ_{13}, θ_{23}, and Δm^2_{31}, and δ. The sign of Δm^2_{31}, i.e. the measurement of mass order, and CP phase of δ will be discussed in detail in [1].

The Super-Kamiokande, IceCube/DeepCore, Minos/Minos+, T2K, and NOvA experiments are in the sensitive energy region for atmospheric and accelerator neutrino oscillation measurement. Charged muons and electrons from CC events of neutrinos on target nucleons are the main detection signal. Muon's sharp Cherenkov rings and electron's fuzzy rings are the main experimental signature in the Super-Kamiokande detector, which is also the far detector of the T2K experiment. Muon's long tracks and electron's short tracks (cascades) are the major experimental signature in the other experiments. Showers from NC events and τ production can also be identified in some cases.

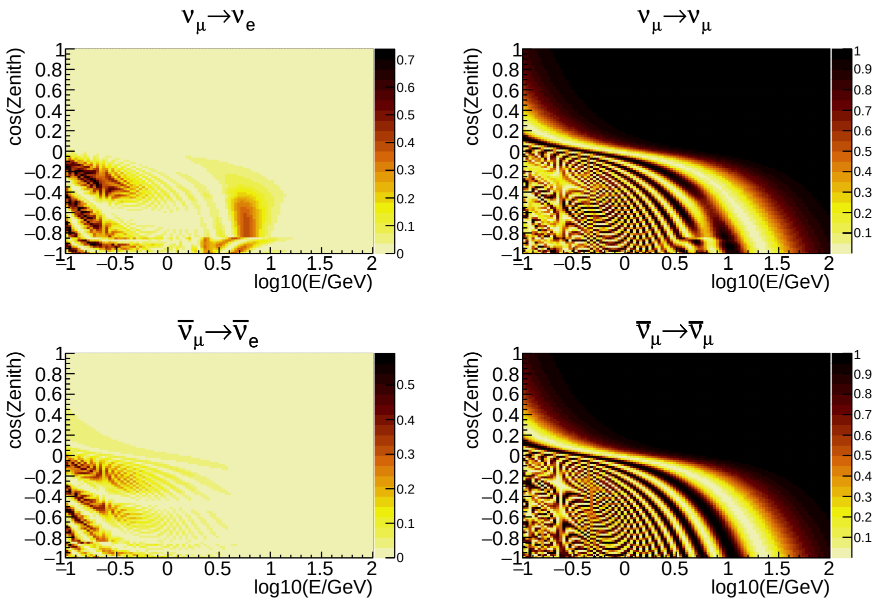

Figure 1: Atmospheric and accelerator ν_μ and $\bar{\nu}_\mu$ oscillation probability, the z axis. $\cos(Zenith) < 0$ is for neutrino coming through the Earth. The plots are generated with $\Delta m^2_{32} > 0$ and $\delta = 0$. Due to limited resolution, some features are artificial.

The new results on θ_{23} and Δm^2_{32} from the atmospheric neutrino analyses of Super-Kamiokande, IceCube/DeepCore, and Minos/Minos+ are summarized in Tab. 3. The results from accelerator neutrino analyses do not show a trivial two-dimensional ellipse confidence interval, so, for details, one must look into references [14], [15], and [16] for T2K, NOvA and MINOS/MINOS+, respectively.

Table 3: The latest θ_{23} and Δm^2_{32} results from the atmospheric neutrino analyses of Super-Kamiokande, Ice Cube/DeepCore, and Minos/Minos+. No error is directly reported by Minos/Minos+.

Experiment	$\sin^2\theta_{23}$	Δm^2_{32} $[10^{-3}\ eV^2]$
Super-Kamiokande [17] (NO)	$0.44^{+0.05}_{-0.02}$	$2.40^{+0.11}_{-0.12}$
IceCube/DeepCore [18]	$0.58^{+0.04}_{-0.13}$	$2.55^{+0.12}_{-0.11}$
Minos/Minos+ [16] (NO)	0.52	2.11

2.4 Global Fit

Not a single neutrino detector can measure all neutrino oscillation parameters due to different energy and baseline regions. A global fit considering all the experimental inputs is necessary to test their compatibility and generate average results. One global fit result is shown in Tab. 4 [19, 20] with pre-Neutrino2020 data. Other global fit results can be found, for example, in [21, 22].

In the global fit [20], we can see the synergy between experiments, for example, 1) in the determination of the octant of θ_{23}, the input of θ_{13} measurement results from reactor neutrino experiments is necessary, and 2) the joint effort of determining $\sin^2\theta_{23}$ and $|\Delta m^2_{31}|$ with accelerator and atmospheric neutrino experiments. Tensions between experiments also exist, for example, the octant result of θ_{23} between the latest octant result of Super-Kamiokande in [8] and the global fit. A more interesting discussion will be in the sector of mass ordering and δ measurement [1].

Table 4: Global fit results for neutrino oscillation parameters from Ref. [19, 20].

Parameter	Best fit $\pm 1\sigma$
Δm^2_{21} [10^{-5} eV^2]	$7.5^{+0.22}_{-0.20}$
$\lvert\Delta m^2_{31}$ [10^{-3} eV^2] (NO)	$2.56^{+0.03}_{-0.04}$
$\lvert\Delta m^2_{31}$ [10^{-3} eV^2] (IO)	2.46 ± 0.03
$\sin^2\theta_{12}/10^{-1}$	3.18 ± 0.16
$\sin^2\theta_{23}/10^{-1}$ (NO)	$5.66^{+0.16}_{-0.22}$
$\sin^2\theta_{23}/10^{-1}$ (IO)	$5.66^{+0.18}_{-0.23}$
$\sin^2\theta_{13}/10^{-1}$ (NO)	$2.225^{+0.055}_{-0.078}$
$\sin^2\theta_{13}/10^{-1}$ (IO)	$2.250^{+0.056}_{-0.076}$
δ/π (NO)	$1.20^{+0.23}_{-0.14}$
δ/π (IO)	1.54 ± 0.13

3. Three+One Generations

Experimentally there are some anomalies against three-generation neutrino oscillation, which include the LSND result, MiniBooNE result, Gallium anomaly, reactor anomaly, and Neutrino-4 result. These features can be explained with sterile neutrinos or they can be simply our mistakes in understanding the experiments or the other underlying physics. Many theoretical and experimental works are in progress. A nice review of the sterile neutrinos can be found in [23]. Talks presented at the conferences Neutrino 2020 and ICHEP 2020 show some of the progress, including the experimental effort of NEOS, STEREO, PROSPECT, DANSS, SoLid, BEST, SBN, JSNS^2, IceCube, ICARUS, MicroBooNE, Daya Bay, Minos+, KATRIN, and so on.

4. Conclusion

In this paper, I summarized the new progress of the short baseline reactor neutrino experiments, the solar neutrino experiments, and the atmospheric and accelerator neutrino experiments. The anomalies in neutrino experiments are briefly mentioned. The results before the ICHEP 2020 conference are collected. Hope to reach a verdict in the near future.

5. Acknowledgement

This work is supported in part by the National Natural Science Foundation of China (Nos. 11620101004, 11475093, and 11235006), the Ministry of Science and Technology of China (No. 2018YFA0404102), the Key Laboratory of Particle & Radiation Imaging (Tsinghua University), and the CAS Center for Excellence in Particle Physics (CCEPP).

References

[1] Atsuko K. Ichikawa. CPV in the neutrino sector. ICHEP 2020 conference, 2020.

[2] D. Adey et al. Measurement of the Electron Antineutrino Oscillation with 1958 Days of Operation at Daya Bay. *Phys. Rev. Lett.*, 121(24):241805, 2018.

[3] F. P. An et al. New measurement of θ_{13} via neutron capture on hydrogen at Daya Bay. *Phys. Rev.*, D93(7):072011, 2016.

[4] Jonghee Yoo. Recent Results from RENO Experiment. Neutrino 2020 conference, 2020.

[5] C. D. Shin et al. Observation of reactor antineutrino disappearance using delayed neutron capture on hydrogen at RENO. *JHEP*, 04:029, 2020.

[6] Thiago Bezerra. New Results from the Double Chooz Experiment. Neutrino 2020 conference, 2020.

[7] John N. Bahcall and Carlos Pena-Garay. Solar models and solar neutrino oscillations. *New J. Phys.*, 6:63, 2004.

[8] Yasuhiro Nakajima. Recent results and future prospects from Super-Kamiokande. Neutrino 2020 conference, 2020.

[9] M. Honda, T. Kajita, K. Kasahara, and S. Midorikawa. Improvement of low energy atmospheric neutrino flux calculation using the JAM nuclear interaction model. *Phys. Rev.*, D83:123001, 2011.

[10] G. D. Barr, T. K. Gaisser, P. Lipari, Simon Robbins, and T. Stanev. A Three - dimensional calculation of atmospheric neutrinos. *Phys. Rev.*, D70:023006, 2004.

[11] Martin Freund. Analytic approximations for three neutrino oscillation parameters and probabilities in matter. *Phys. Rev.*, D64:053003, 2001.

[12] Sanjib Kumar Agarwalla, Yee Kao, and Tatsu Takeuchi. Analytical approximation of the neutrino oscillation matter effects at large θ_{13}. *JHEP*, 04:047, 2014.

[13] M. Jiang et al. Atmospheric Neutrino Oscillation Analysis with Improved Event Reconstruction in Super-Kamiokande IV. *PTEP*, 2019(5):053F01, 2019.

[14] Laura Munteanu. Neutrino Oscillation Results from the T2K Experiment. ICHEP 2020 conference, 2020.

[15] Alex Himmel. New Oscillation Results from the NOvA Experiment. Neutrino 2020 conference, 2020.

[16] P. Adamson et al. Precision Constraints for Three-Flavor Neutrino Oscillations from the Full MINOS+ and MINOS Dataset. *Phys. Rev. Lett.*, 125(13):131802, 2020.

[17] Volodymyr Takhistov. Atmospheric Neutrino Oscillations with Super-Kamiokande. ICHEP 2020 conference, 2020.

[18] M. G. Aartsen et al. Measurement of Atmospheric Tau Neutrino Appearance with IceCube DeepCore. *Phys. Rev.*, D99(3):032007, 2019.

[19] Mariam Tòrtola. Global fits to neutrino masses and mixings. ICHEP 2020 conference, 2020.

[20] P. F. de Salas et al. 2020 Global reassessment of the neutrino oscillation picture. *arXiv:2006.11237*, 2020.

[21] Ivan Esteban et al. Global analysis of three-flavour neutrino oscillations: synergies and tensions in the determination of θ_{23}, δ_{CP}, and the mass ordering. *JHEP*, 01:106, 2019.

[22] Francesco Capozzi et al. Global constraints on absolute neutrino masses and their ordering. *Phys. Rev.*, D95(9):096014, 2017. [Addendum: Phys. Rev.D101,no.11,116013(2020)].

[23] K. N. Abazajian et al. Light Sterile Neutrinos: A White Paper. *arXiv:1204.5379*, 2012.